Bioactive Materials 24 (2023) 376–386

Contents lists available at ScienceDirect

Bioactive Materials

journal homepage: www.keaipublishing.com/en/journals/bioactive-materials

Zwitterionic betaines over HEPES as the new generation biocompatible pH buffers for cell culture

Peiming Liu [a,1], Jin Sun [a,1], Wan Peng [a], Yahui Gu [a], Xiaoxue Ji [a], Zhi Su [a], Pingsheng Liu [a,*], Jian Shen [a,b,**]

[a] Jiangsu Collaborative Innovation Center of Biomedical Functional Materials, Jiangsu Key Laboratory of Bio-functional Materials, School of Chemistry and Materials Science, Nanjing Normal University, Jiangsu, 210023, China
[b] Jiangsu Engineering Research Center of Interfacial Chemistry, School of Chemistry and Chemical Engineering, Nanjing University, Jiangsu, 210093, China

ARTICLE INFO

Keywords:
Good's buffers
Zwitterionic betaines
ROS conversion
Cellular functions
Biocompatibility

ABSTRACT

Good's buffers have been widely applied in cell/organ culture over the past half a century as biocompatible pH stabilizers. However, the emergence of severe adverse effects, such as cellular uptake, lysosomal autophagic activation, and visible light-induced cytotoxicity, raises serious questions over its biocompatibility while underlying mechanism was unclear. Here we report that riboflavin (RF, component of cell culture medium) generates $^1O_2$, ·OH, and $O_2^{\bullet-}$ under visible light exposure during regular cell manipulation. These short half-life reactive oxygen species (ROS) react with tertiary amine groups of HEPES, producing 106.6 μM of H_2O_2. Orders of magnitude elevated half-life of ROS in the medium caused severe cytotoxicity and systematic disorder of normal cell functions. We have further designed and validated zwitterionic betaines as the new generation biocompatible organic pH buffers, which is able to completely avoid the adverse effects that found on HEPES and derivate Good's buffers. These findings may also open a new avenue for zwitterionic betaine based materials for biomedical applications.

1. Introduction

Stable pH is extremely important for the culture of normal and pathological cells [1,2]. Minor pH variation of the culture medium can significantly affect the cellular fate and behavior [2–4]. Incubator with CO_2–$NaHCO_3$ as the buffering system is the current standard facility for cell culture. However, cells have to be removed out from incubators for diverse essential bench manipulations. To minimize pH variation of cell culture mediums during bench manipulations, Good and colleagues proposed a serial of organic substances for biological research in 1966 [5]. These small molecular substances possess both positive and negative structures that can simultaneously act as conjugate acid and conjugate base (Fig. S1A) to enable a stable pH for the cell culture mixture for days outside the incubator. Therefore, it offers enough time for diverse bench manipulations. Moreover, in comparison to conventional inorganic buffers, Good's buffers have been shown with multiple advantages: no participation in biological reactions, ignorable metal chelating capability, no cell membrane permeability and no cytotoxicity to normal mammalian cells [6,7]. These merits have made Good's buffers as the most popular buffering substances for cell/tissue culture, virus identification, vaccine manufacture, and protein/tissue storage over the past half a century [2,5]. Nevertheless, emerging severe adverse effects in cell/tissue cultures have been reported. For example, 4-(2-hydroxyethyl)-1-piperazineethanesulfonic acid (HEPES) was found to be endocytosed by cells [8]. RPMI 1640 medium supplied with HEPES (25 mM) resulted in significant cytotoxicity under visible light [9], while the presence of HEPES in the culture medium clearly up-regulate lysosomal-autophagic aggravation and inflammatory signaling of the cells [10]. However, the underlying mechanism of these emerging severe adverse effects associated with HEPES remains unclear.

ROS, including H_2O_2, $^1O_2$, ·OH, and $O_2^{\bullet-}$ (Table 1), play essential roles in cell signaling for it mediates diverse cell functions where redox

Peer review under responsibility of KeAi Communications Co., Ltd.

* Corresponding author.
** Corresponding author. Jiangsu Collaborative Innovation Center of Biomedical Functional Materials, Jiangsu Key Laboratory of Bio-functional Materials, School of Chemistry and Materials Science, Nanjing Normal University, Jiangsu, 210023, China.
E-mail addresses: liups@njnu.edu.cn (P. Liu), jshen@njnu.edu.cn (J. Shen).
[1] These authors contributed equally to this work.

https://doi.org/10.1016/j.bioactmat.2022.12.028
Received 25 July 2022; Received in revised form 25 December 2022; Accepted 26 December 2022

Table 1
Half-life and reaction radius of different reactive oxygen species.

radicals	half-life[a]	reaction radius	ref.
singlet oxygen ($^1O_2$)	~48 ns	<20 nm[b]	[20–22]
superoxide ($O^{\bullet 2-}$)	~1 μs	limited[b]	[23]
hydroxyl radical (•OH)	~1 ns	limited[b]	[24]
hydrogen peroxide (H_2O_2)	long half-life time	can pass through cell membranes freely	[24]

[a] may slightly varied depend on solvent.
[b] Normally acts where it is generated.

signaling is involved [11–13]. However, it is considered to be a "necessary evil" [12] for cell signaling because the excessive ROS clearly damages DNA, protein and lipid of cells [14]. Therefore, the level of intracellular H_2O_2 is tightly regulated within the range of 0.001–0.7 μM for normal mammalian cells [15], while that of extracellular H_2O_2 is up to 4 μM [15,16]. Previous studies have shown that oxidative compounds can induce H_2O_2 formation in the presence of HEPES or related tertiary amines in PBS [17], the presence of RF in the cell culture medium can generate ROS under light irradiation [18], and the over-express of flavin-containing oxidase was proposed to trigger light-induced production of H_2O_2 in mammalian cells [19]. Therefore, we hypothesis that the severe adverse effects found on HEPES might be associated with the potential abnormal ROS production in the HEPES buffered mediums.

To test this hypothesis, we attempt to systematically investigate the extracellular and intracellular ROS production in cell culture medium with/without HEPES, specify the source of ROS, verify the consequent disordering of cell functions, and further propose potential alternative buffering substance that is able to eliminate the severe adverse effects found on HEPES.

2. Materials and methods

2.1. Synthesis and characterization of zwitterionic monomers

2-(methacryloyloxy)ethyl]dimethyl-(3-sulfopropyl)ammonium hydroxide (SBMA) monomer was synthesized as follows: 1, 3-Propane sulfone (1, 3-PS, 96 mmol) in 100 mL anhydrous chloroform was added dropwise to a solution of 2-(dimethylamino)ethyl methacrylate (DMAEMA, 80 mmol in 200 mL of dried chloroform). The mixture was stirred under a nitrogen atmosphere at 30 °C for 48 h. The resulting mixture was filtered and washed with 100 mL of diethyl ether. The product was dried under vacuum to obtain the final SBMA monomer. The monomer was kept at 2-8 °C before further use. ^{1}H NMR (400 MHz): 6.16 (s, 1H, =CH2), 5.78 (s, 1H, =CH2), 4.64 (t, 2H, OCH_2), 3.83 (t, 2H, CH_2N), 3.59 (t, 2H, NCH_2), 3.22 (s, 6H, NCH_3), 2.97 (t, 2H, CH_2SO_3), 2.28 (t, 2H, $–CH_2$-), 1.94 (s, 3H, $=CCH_3$).

2-methacryloyloxyethyl phosphorylcholine (MPC) was purchased from Nature's Joy (Nanjing, China). ^{1}H NMR (400 MHz): 6.11 (s, 1H, =CH), 5.68 (s, 1H, =CH), 4.32 (t, 2H, $COOCH_2$), 4.22 (t, 2H, OCH_2), 4.10 (t, 2H, CH_2O), 3.59 (t, 2H, CH_2N), 3.14 (s, 9H, NCH_3), 1.87 (s, 3H, $=CCH_3$).

3-(2-(methacryloyloxy)ethyl dimethylammonio) propanoate (CBMA) monomer was prepared according to the published protocol [25]: briefly, β-propiolactone (6 mmol) in 5 mL anhydrous acetone was added dropwise to a solution of DMAEMA (0.79 g, 5 mmol, in 25 mL dried acetone). The resulting mixture was stirred under a nitrogen atmosphere at 15 °C for 5 h. The resulting mixture was filtered, washed with 100 mL of diethyl ether and dried under vacuum to obtain the final CBMA monomer. The monomer was kept at 2-8 °C before further use. ^{1}H NMR (400 MHz): 6.15 (s, 1H, $=CH_2$), 5.77 (s, 1H, $=CH_2$), 4.64 (t, 2H, OCH_2), 3.79 (t, 2H, CH_2N), 3.67 (t, 2H, NCH_2), 3.19 (s, 6H, NCH_3), 2.73 (t, 2H, CH_2COO), 1.93 (s, 3H, $=CCH_3$).

2.2. Synthesis of zwitterionic polymers

The preparation of the zwitterionic homo-polymers was adapted from the published protocol [26]. Briefly, zwitterionic monomer was dissolved in distilled water forming a 1 mol/L solution, which was followed by the addition of ammonium persulfate (APS, 1: 14 to monomer in mol ratio) and *N,N,N′,N′*-tetramethylethylenediamine (TEMED, 1: 93 to monomer in mol ratio). The polymerization was carried out for 24 h under 37 °C. The resulting mixture was dialyzed against water to remove the residues using dialysis tubing (MWCO: 5000 Da). Zwitterionic polymers were obtained after freeze drying. ^{1}HNMR of pSBMA, pMPC and pCBMA were recorded on a Bruker spectrometer using deuterated water as a solvent. Molecular weights of three zwitterionic polymers were determined with gel permeation chromatography (GPC) using Shimadzu LC solution, trizma buffer as the eluent and polyethylene glycol as the calibrating standard.

In order to avoid the influence of the catalyst residue on the cytocompatibility of the zwitterionic polymers, a UV induced polymerization was performed to synthesize the zwitterionic polymers. Typically, 7 mmol of monomer was dissolved in 6 mL of ultrapure water, which was followed by the addition of 350 μL of 2,2-azobis[2-methyl-N-(2-hydroxyethyl)propionamide] (VA-086, 2% w/v) solution. The mixture was irradiated by a 365 nm UV light for 10 min at room temperature. The resulting mixture was dialyzed (MWCO: 5000 Da) against water for 6 days before freeze drying.

2.3. Synthesis and characterization of small molecular betaines

3-(Butyldimethylammonio)propane-1-sulfonate (S-4) was synthesized as follows: *N, N*-dimethylaminobutane (60 mmol) was added dropwise to a solution of 1, 3-propane sulfone (1,3-PS, 60 mmol in 15 mL ethyl acetate). The mixture was stirred at 55 °C for 3 h. The resulting mixture was filtered and washed with dry ethyl acetate. After dried under vacuum, a white powder of S-4 was obtained. ^{1}H NMR (400 MHz): 3.47 (t, 2H, NCH_2), 3.34 (t, 2H, CH_2N), 3.08 (s, 6H, NCH_3), 2.97 (t, 2H, CH_2SO_3), 2.20 (t, 2H, $–CH_2$-), 1.74 (t, 2H, $–CH_2$-), 1.37 (t, 2H, $–CH_2$-), 0.94 (t, 3H, $–CH_3$).

3-(3-hydroxypropyl)dimethylammonio propane-1-sulfonate (S–OH) was synthesized as follows: 1, 3-PS (143 mmol in 10 mL acetonitrile) was added dropwise to a solution of 3-dimethylamino-1-propanol (150 mmol in 125 mL acetonitrile). The mixture was stirred at 55 °C for 7 h. The resulting mixture was filtered and washed with dry acetonitrile. After dried under vacuum, a white powder of S–OH was obtained. ^{1}H NMR (400 MHz): 3.69 (t, 2H, $–CH_2OH$), 3.49 (t, 4H, CH_2N), 3.11 (s, 6H, NCH_3), 2.99 (t, 2H, CH_2SO_3), 2.25 (t, 2H, $–CH_2$-), 2.03 (t, 2H, $–CH_2$-).

3-(butyldimethylammonio)propanoate (C-4) was synthesized as follows: *β*-propiolactone (6 mmol) in 5 mL anhydrous acetone was added dropwise to a solution of *N, N*-dimethylaminobutane (5 mmol, in 25 mL dried acetone). The reaction mixture was stirred at room temperature for 24 h. The resulting mixture was filtered, washed with 100 mL of diethyl ether and dried under vacuum to obtain C-4 white powder. ^{1}H NMR (400 MHz): 3.54 (t, 2H, NCH_2), 3.29 (t, 2H, CH_2N), 3.05 (s, 6H, NCH_3), 2.66 (t, 2H, CH_2CO_2), 1.75 (t, 2H, $–CH_2$-), 1.39 (t, 2H, $–CH_2$-), 0.96 (t, 3H, $–CH_3$).

2-(trimethylammonio)acetate (betaine) was purchased from Tansoole (Shanghai, China). ^{1}H NMR (400 MHz): 3.89 (s, 2H, NCH_2CO_2), 3.25 (s, 9H, NCH_3).

2.4. Visible light-induced H_2O_2 formation of the buffers

Fourteen RPMI 1640 mediums with different buffers or varied concentration of buffers (RPMI 1640 + 25 mM HEPES, RPMI 1640 + 25 mM pSBMA, RPMI 1640 + 25 mM pMPC, RPMI 1640 + 25 mM pCBMA, RPMI 1640 + 50 mM HEPES, RPMI 1640 + 50 mM pSBMA, RPMI 1640 + 25 mM Tris, RPMI 1640 + 25 mM TES, RPMI 1640 + 25 mM Tricine, RPMI 1640 + 25 mM MOPSO, RPMI 1640 + 25 mM POPSO, RPMI 1640

+ 25 mM MES, and RPMI 1640 + 25 mM BES) were prepared. All the mediums were sterilized by passing through a 0.45 μm polyethersulfone membrane filter (Millipore) and stored under dark conditions at 4 °C before use.

Visible light-induced H_2O_2 formation of the buffers was measured via hydrogen peroxide assay kit (Beyotime, China). Briefly, 1 mL of each culture medium (n = 3) was transferred into a 24-well cell culture plate (Corning) and put in the clean bench with the bench visible light turned on (18 W, 1 mW/cm^2) at a distance of 30 cm for 0.5 h, 1 h, 3 h, respectively. Then, 50 μL of each resulting medium was mixed with 100 μL of detection reagent in a 96-well plate. The optical density at 570 nm was recorded. In the meantime, the optical densities of another batch of mediums that were in dark conditions were also measured as the control for each group. The concentration of H_2O_2 formed in the solution was calculated from the standard curve.

The net concentration (N) of the H_2O_2 generated from various culture media was calculated according to the equation:

$$N = N_{light} - N_{dark} \quad (1)$$

where N_{light} and N_{dark} are the concentrations of H_2O_2 generated in the culture mediums that were exposed to visible light from a clean bench and stored in dark conditions, respectively.

2.5. Simulated sunlight-induced H_2O_2 formation of the buffers

Five buffered culture mediums, RPMI 1640 + 25 mM HEPES, RPMI 1640 + 25 mM S-4, RPMI 1640 + 25 mM S–OH, RPMI 1640 + 25 mM C-4, RPMI 1640 + 25 mM Betaine, and pristine RPMI 1640 without HEPES or zwitterions were prepared. Culture mediums were sterilized by passing through a 0.45 μm polyethersulfone membrane filter (Millipore) and stored under dark conditions at 4 °C before use.

Simulated sunlight-induced H_2O_2 formation of the buffers was measured via hydrogen peroxide assay kit (Beyotime, China). Briefly, 100 μL of each culture medium (n = 3) was transferred into a 96-well cell culture plate (Tansoole) with the simulated sunlight turned on (100 mW/cm^2, 5 min), respectively. After that, 50 μL of each resulting medium was mixed with 100 μL of detection reagent in a 96-well plate and the optical absorbance at 570 nm was recorded on a microplate reader. The H_2O_2 concentration was calculated according to Equation (1).

2.6. Cellular uptake of the buffers

The cellular uptake behavior of the buffers was evaluated by ^{1}H NMR and mass spectrometry measurement (MS) analysis of the intracellular matrix. The NMR testing buffer was firstly prepared according to the published protocol [27]. Briefly, 0.39 g of $NaH_2PO_4{\cdot}2H_2O$ was dissolved in 20 mL of ultrapure water. The pH of the solution was adjusted to 7.0 by NaOH solution. Ultrapure water was added to the solution to reach a final volume of 25 mL. The solution was frozen under −20 °C and lyophilized to obtain NMR buffer salts. The salts were then dissolved in a small amount of D_2O and the resulting solution was lyophilized again. The resulting buffer salt was dissolved in D_2O to a final volume of 25 mL. The NMR testing buffer was stored at −20 °C before use.

Hela cells were cultured in DMEM medium (Boster, China) supplemented with 10% fetal bovine serum and 1% penicillin/streptomycin at 37 °C in a humidified atmosphere with 5% CO_2 for 3 days. Buffered DMEM mediums that contained an additional 25 mM of HEPES, pSBMA, pMPC, pCBMA, S-4, S–OH, C-4 or Betaine were prepared and sterilized by passing through a 0.45 μm PVDF membrane filter (Millipore). Cell culture medium was then changed from DMEM medium to HEPES/DMEM, pSBMA/DMEM, pMPC/DMEM, and pCBMA/DMEM, S-4/DMEM, S–OH/DMEM, C-4/DMEM and Betaine/DMEM, respectively. After an additional 24 h incubation, cells were washed three times with 3 mL of ice-cold PBS. Then, about 10^6 of Hela cells harvested from each culture conditions were washed with sterile PBS twice (re-suspend the cells in 1 mL of sterile PBS and then isolate it by centrifugation).

To extract the metabolite from the cells, a 900 μL of chloroform/methanol (6/3, v/v) solution was mixed with the cell pellet. The mixture sonicated four times (each for 3 s) using a sonifier to damage the cell membrane. Then the mixture was centrifuged at 15,000 rpm for 20 min under 4 °C. The supernatant (~1 mL) was collected and lyophilized [8].

For ^{1}HNMR measurement, cell metabolite extract was dissolved in 300 μL NMR testing buffer. The ^{1}H NMR spectra were recorded on a Bruker 400 AVANCE III spectrometer with 512 scans.

For mass spectrometry measurement (MS), cell metabolite extract was dissolved in mixed solution of methanol and H_2O (1:3 by volume). The MS spectra were recorded on a DART-SVP (Ion Sense Inc., Saugus, MA, United States) ion source coupled to an Orbitrap Fusion Lumos mass spectrometer (Thermo Fisher Scientific, United States).

2.7. ROS imaging of cells

The intracellular ROS was measured by the DCFH-DA assay kit (Beyotime, China). To test the effect of ROS in RAW 264.7 cells, briefly, RAW 264.7 cells were seeded into the 24-well cell culture plate at a density of about 10^4 cells per well and incubated with RPMI 1640 medium overnight at 37 °C and 5% CO_2. Then medium was changed to 25 mM HEPES/RPMI 1640, 25 mM pSBMA/RPMI 1640, respectively and cells were incubated for 24 h. Then the culture plate was directly put in the clean bench with the bench visible light turned on (1 mW/cm^2) for 1 h. The cells were carefully rinsed twice with PBS and incubated with 10 μM DCFH-DA in FBS-free RPMI 1640 medium for 20 min in the dark. The cells were carefully rinsed with fresh cell culture medium and the intracellular ROS levels were determined by confocal laser microscopy with excitation wavelength at 488 nm.

To test the effect of ROS in L-02 cells, briefly, L-02 cells were seeded in 35 mm confocal culture dishes (Wuxi NEST Biotechnology Co., Ltd, China) and incubated with RPMI 1640 medium overnight at 37 °C and 5% CO_2. Then the medium was changed to 25 mM HEPES/RPMI 1640, 25 mM POPSO/RPMI 1640, 25 mM MOPSO/RPMI 1640, 25 mM Tricine/RPMI 1640, 25 mM pSBMA/RPMI 1640, 25 mM pCBMA/RPMI 1640, 25 mM pMPC/RPMI 1640, respectively and cells were incubated for 24 h. Then the culture dishes were put in the clean bench with the bench visible light turned on (1 mW/cm^2) for 3 h. Cells were stained and photographed according to the above steps for RAW 264.7 cells.

To test the intracellular ROS in L-02 cells, after incubating with different buffer mediums for 24 h, the medium was changed to RPMI 1640 and the culture plate was directly put in the clean bench with the bench visible light turned on (1 mW/cm^2) for 3 h. The intracellular ROS levels were determined with confocal laser microscopy with excitation wavelength at 488 nm.

To test the effect of ROS in L-02 cells induced by simulated sunlight, briefly, L-02 cells were seeded into the 24-well cell culture plate and allowed to grow in pristine RPMI 1640 medium for 24 h. Then the medium was changed to 25 mM HEPES/RPMI 1640, 25 mM S-4/RPMI 1640, 25 mM S–OH/RPMI 1640, 25 mM C-4/RPMI 1640, 25 mM Betaine/RPMI 1640, respectively for another 24h. After staining the cells, the culture plates were put under the simulated sunlight with light turned on (100 mW/cm^2) for 5min, respectively, and photographed by inverted fluorescence microscope (Nikon, N Storm).

2.8. Lysosomal activation of cells by buffers

Ana-1 cells (Cell Bank of the Chinese Academy of Sciences, Shanghai, China) were cultured in 10 mL of RPMI 1640 medium (Boster, China) supplemented with 10% fetal bovine serum (ScienCell) and 1% penicillin/streptomycin. Cells were harvested and were re-suspended in a fresh medium. Equal amounts of the cell suspension were transferred to the glass bottom cell culture dish (NEST, China) and were cultured in RPMI 1640 mediums containing 25 mM of HEPES, pSBMA, pMPC or

pCBMA for 24 h. Cells cultured in regular RPMI 1640 medium were served as the control. After incubation, cells were rinsed gently with fresh medium, stained with 50 nM LysoTracker Red DND-99 (Beyotime, China, 5 min), washed with fresh medium, and imaged by confocal microscope (Nikon, N Storm).

RAW 264.7 cells were cultured in 10 mL of DMEM medium (Boster, China) supplemented with 10% fetal bovine serum and 1% penicillin/streptomycin. Cells were harvested and were re-suspended in a fresh medium. Equal amounts of the cell suspension were transferred to the 24-well cell culture plate and were cultured in DMEM mediums containing 25 mM of HEPES, S-4, S–OH, C-4 or Betaine for 24 h. Cells cultured in regular DMEM medium were served as the control. After the culture, cells were rinsed gently with fresh medium, stained with 50 nM LysoTracker Red DND-99 (Beyotime, China, 5 min), washed with fresh medium, and imaged by inverted fluorescence microscope (Nikon, N Storm).

2.9. Immunofluorescence

RAW264.7 cells (3×10^5 cells in 3 mL of RPMI 1640 medium in each well) were cultured in a 6-well cell culture plate with glass coverslip in each well for 24 h. The mediums in each well were replaced with 2 mL of fresh mediums (RPMI 1640, RPMI 1640 with 25 mM of HEPES, and RPMI 1640 with 25 mM of pMPC) which were exposed to regular visible light in clean bench for 3 h in advance, respectively. After further 4 h incubation, cells on glass coverslips were fixed in 4% paraformaldehyde (Beyotime, P0099) for 10 min at room temperature. Then, cells were rinsed in ice-cold PBS, treated with PBS containing 0.15% Triton (× 100) for 10 min, washed in PBS, and incubated in blocking buffer (Beyotime, P0220) for 10 min. The cells were firstly stained with diluted primary antibody for TFE3 (Affinity, AF7015) overnight at 4 °C. After washed in PBS, cells were incubated with Alexa Fluor 488-labeled Goat Anti-Rabbit IgG(H + L) (Beyotime, A0423) for 1 h in dark condition, washed in PBS and then stained in DAPI solution (Beyotime, C1006) for 5 min in dark condition. After washed with PBS, each glass coverslip was mounted with a drop of antifade mounting medium (Beyotime, P0126). Representative images were captured with a Confocal Nikon with a 100× objective and an excitation wavelength of 488 nm.

2.10. Cytotoxicity assay

Cytotoxicity of the several representative Good's buffers (HEPES, MOPSO, POPSO, and Tricine) and zwitterion polymers containing mediums on five type of cells (L-02, RAW264.7, NB4, Hela, and A549 cells) in addition to the previous experiments on cells) was evaluated by the Cell Counting Kit-8 (CCK-8) assay. Briefly, pristine RPMI 1640 medium and RPMI 1640 containing 25 mM of different buffer culture mediums, pSBMA, pCBMA, or pMPC were exposed to regular visible bench light for 3 h. Afterwards, 100 μL of each resulting medium were placed into 96-well microplates, and 100 μL cells suspension (1×10^5 cell/mL) added into each well. Cells cultured with the corresponding medium that were stored under dark conditions were set as the control for each group. After 24-h's incubation at 37 °C, the medium in each well was replaced by 200 μL of fresh RPMI 1640 and 20 μL of CCK-8 reagent. Cells were cultured for an additional 4 h incubation, the absorbance (at 450 nm) of the medium from each well was recorded on a microplate reader. Cell viability was determined via the following equation:

$$\text{Cell viability } (\%) = (OD_{\text{experimental group}}/OD_{\text{control group}}) \times 100\% \quad (2)$$

Cytotoxicity of the HEPES and zwitterions containing mediums was evaluated by the Cell Counting Kit-8 (CCK-8) assay. Briefly, pristine RPMI 1640 medium and RPMI 1640 containing 25 mM of HEPES, S-4, S–OH, C-4 or Betaine were exposed to simulated sunlight for 5 min. Afterwards, 100 μL of each resulting medium were placed into 96-well microplates, and 100 μL cells suspension (1×10^5 cell/mL) added into each well. Cells cultured with the lighted RPMI 1640 medium were set as the control. After 24-h's incubation at 37 °C, cell viability of each buffered medium was detected according to the above steps for visible light measurements.

2.11. LIVE/DEAD staining assays

The viability of L-02 cells was evaluated with the LIVE/DEAD Assay. L-02 cells were seeded in 35 mm confocal culture dishes (Wuxi NEST Biotechnology Co., Ltd, China) and allowed to grow in pristine RPMI 1640 medium for 24 h. Then, the culture media were replaced by visible light exposed mediums that contained 25 mM of HEPES or zwitterion polymers. After an additional 24 h culture, cells were stained with the LIVE/DEAD kit according to vender's protocol. The live/dead images of cells were recorded by laser confocal microscopy (Nikon, N Storm).

2.12. Apoptosis assays

Apoptosis of cells that cultured in HEPES and zwitterion polymers (pMPC) containing mediums was evaluated by the Annexin V-EGFP Apoptosis Detection Kit (Beyotime). Briefly, 1 mL of L-02 cells suspension (3×10^4 cell/mL in pristine RPMI 1640) was seeded into each well of a 24-well cell culture plate. After 24 h' culture, the medium in each well were replaced by fresh RPMI 1640 mediums that containing 25 mM of HEPES and pMPC, respectively. Immediately, the conditioned mediums with cells were exposed to the regular visible bench light (Fig. S1B) for 1 h and 3 h, respectively. After additional 24 h' incubation at 37 °C, the cells were stained with the Annexin V-EGFP Apoptosis Detection Kit according to the vendor' protocol (Beyotime, Annexin V-EGFP Apoptosis Detection Kit). The fluorescence of the cells was imaged with a fluorescence microscope.

2.13. Electron spin resonance (ESR) spectroscopy measurements

The visible light induced generation of ROS of riboflavin solutions with/without HEPES were evaluated by ESR spectroscopy. 2,2,6,6-tetramethylpiperidine (TEMP, 50 mM) was used as a spin trap to detect $^1O_2$, and 5,5-dimethyl-1-pyrroline-N-oxide (DMPO, 100 mM) was used to trap $O_2^{\bullet-}$ and ·OH. Typically, 200 μL of sample suspension (riboflavin: 20 μM) and 600 μL of the capture agent were irradiated under a 300 W Xe lamp (120 mW/cm^2) for 5 min. After that, 200 μL of the freshly prepared mixture was added to a quartz EPR tube and then sealed. The ESR spectra was acquired by inserting the tube into the spectrometer cavity.

2.14. Buffering capability tests

To test the buffering capability of pSBMA, pMPC, pCBMA and HEPES, 0.21 M of pSBMA, pMPC, pCBMA and HEPES stock solutions (with 0.1 M NaCl) were prepared and the pH was adjusted to 7.00. The concentrations of the zwitterionic polymers were calculated according to the zwitterionic repeat units in the polymers. Acidic standard solution (pH = 3.00) and the basic standard solution (pH = 9.00) were prepared with 0.1 M HCl or NaOH solution, respectively. Typically, acidic or basic standard solution was loaded into the syringe and injected into 8 mL of each stock solution via pumping (WH-SP-02, Suzhou Wenhao Microfluidic Technology Co., Ltd.) at a constant rate (200 μL/min). Real-time pH value was recorded every 2 min by pH meter (PI5100, Alalis Instruments Technology (Shanghai) Co., Ltd.). The 0.1 M NaCl solution without any buffering reagent was set as the control.

To test the intrinsic buffering capacity of pCBMA and HEPES, the pCBMA and HEPES stock solutions (0.21 M) were prepared without pH adjustment. Real-time pH values of the two buffering solutions were recorded as per the methods described above.

To test the buffering capability of S-4, S–OH, C-4, Betaine and HEPES, 0.1 M of S-4, S–OH, C-4, Betaine and HEPES stock solutions

(with 0.1 M NaCl) were prepared and the pH was adjusted to 7.00. Acidic standard solution (pH = 4.00) was prepared with 0.1 M HCl solution. Typically, acidic or basic standard solution was loaded into the syringe and injected into 8 mL of each stock solution via pumping (WH-SP-02, Suzhou Wenhao Microfluidic Technology Co., Ltd.) at a constant rate (200 μL/min). Real-time pH value was recorded every minute by pH meter (962244, Shanghai INESA Scientific Instrument Co., Ltd.). The 0.1 M NaCl solution without any buffering reagent was set as the control. The buffering capacity of each buffer was calculated according to the Van Slyke buffer capacity (β) equation [28,29]:

$$\beta = -\frac{dA}{dpH} \text{ or } \beta = \frac{dB}{dpH} \quad (3)$$

where A and B are the number of moles of strong base and strong acid, respectively [30].

2.15. pH variation in buffered medium

Firstly, the DMEM powder (D2902) was purchased from Sigma-Aldrich and dissolved in sterilized water to form the DMEM medium. Then, DMEM +10% FBS, 25 mM NaHCO3/DMEM +10% FBS, 25 mM HEPES/DMEM +10% FBS, 25 mM pCBMA/DMEM +10% FBS and 50 mM pCBMA/DMEM +10% FBS were prepared and sterilized by passing through a 0.45 μm polyethersulfone membrane filter (Beyotime). All the pH was adjusted to 7.20 using NaOH or HCl solution before adding to the culture flask. Then, 4 mL of Hela cells (50 000 per mL) were cultured in sealed culture flasks over 24 h, and the medium were replaced to corresponding DMEM media, respectively. At the time point, the media were taken out and the pH was tested using pH meter. Cell morphology was captured by a microscope (Nikon, ECLIPSE Ti).

3. Results and discussion

3.1. Extracellular ROS production in RPMI 1640 mediums associated with HEPES and zwitterionic polybetaines

To investigate the extracellular ROS production in HEPES buffered cell culture medium, RPMI 1640 medium supplemented with 25 mM of HEPES (Fig. 1A) was exposed to the visible light of clean bench (Fig. S1B). About 9.7 μM of H_2O_2 was detected in pristine RPMI 1640 medium without HEPES (Fig. 1B) after 3h′s exposure, mainly due to the RF component (0.2 mg/L) is a photosensitizer [18]. Further specific electron spin resonance (ESR) evaluation on RF solutions revealed the presence of three primary ROS ($^1O_2$, ·OH, and $O_2^{\bullet-}$) during the regular in-door visible light exposure (Fig. 1C and Fig. S2). Surprisingly, significantly decreased $^1O_2$ and ·OH signals (by 93.2% and 73.4%, respectively) signals were detected in HEPES buffered medium (Fig. 1C). Instead, more than 10-fold increased H_2O_2 (106.6 μM) was detected (Fig. 1B) with exposure time and concentration dependent manners (Fig. 1D &E).

Previously, Kirsch et al. created a model and tested the possibility that utilize nitric oxide (·NO) and $O_2^{\bullet-}$ as the precursor oxidants to trigger H_2O_2 formation in PBS. They found that the amount of H_2O_2 was increased from 15 μM to 190 μM with the presence of HEPES, and proposed the mechanism by drawing attention to the tertiary amine structures, which act as the electron donating group accelerating the H_2O_2 formation in the presence of precursor oxidants [17]. Theoretically, the massive primary ROS species ($^1O_2$, ·OH, and $O_2^{\bullet-}$) detected in the mediums that originated from RF under visible light exposure (Fig. 1C and Fig. S2) can also act as the oxidants to trigger the H_2O_2 formation in the presence of HEPES (Fig. 1F).

Beyond HEPES, we further tested the abnormal H_2O_2 formation in RPMI 1640 mediums that supplied with seven additional typical Good's buffers (Tris, TES, Tricine, MOPSO, POPSO, MES, and BES, Fig. 2A). As quantified by H_2O_2 quantification kit, about 91.2–156.7 μM of H_2O_2 were formed in four tertiary amine groups (MOPSO, POPSO, MES, and BES), and about 60 μM of H_2O_2 were formed in two secondary amine groups (TES and Tricine), while no obvious up-regulated H_2O_2 formation in the mediums that supplied with Tris under identical condition (Fig. 2B). In light of the wide presence of tertiary amine and secondary amine structures in Good's buffers (Fig. S1A), the abnormal H_2O_2 formation in the cell culture medium supplied with Good's buffers is anticipated to be general.

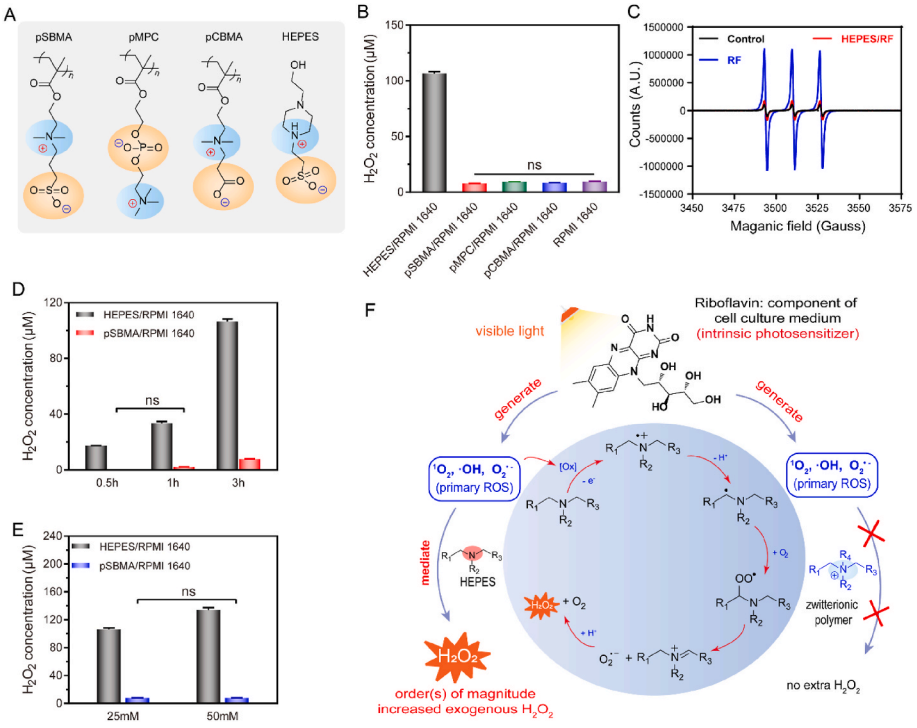

Fig. 1. Extracellular ROS production in RPMI 1640 mediums supplied with identical concentration of HEPES and zwitterionic polybetaines under visible light illumination. (A) Chemical structure of three zwitterionic polybetaines (pSBMA, pMPC, and pCBMA) and HEPES. **(B)** Amount of H_2O_2 produced in RPMI 1640 mediums supplied with 25 mM of HEPES or zwitterionic polybetaines under visible light illumination of the ordinary clean bench (1 mW/cm^2) without cells. RPMI 1640 medium without buffer was set as the negative control. Pairwise comparisons are statistically significant unless denoted as "ns" (not significant) as determined by One-way ANOVA multiple comparison tests. **(C)** ESR spectroscopy of $^1O_2$ detected in RF solutions that irradiated by simulated sunlight (120 mW/cm^2) for 5 min. TEMP was used as a spin trap to detect $^1O_2$. **(D & E)** H_2O_2 formation in RPMI 1640 mediums that buffered by HEPES or pSBMA as a function of visible light-exposure time and concentration of buffers. **(F)** Schematic illustration of mechanism of H_2O_2 production in the medium with the present of quaternary amine or tertiary amine buffering substances.

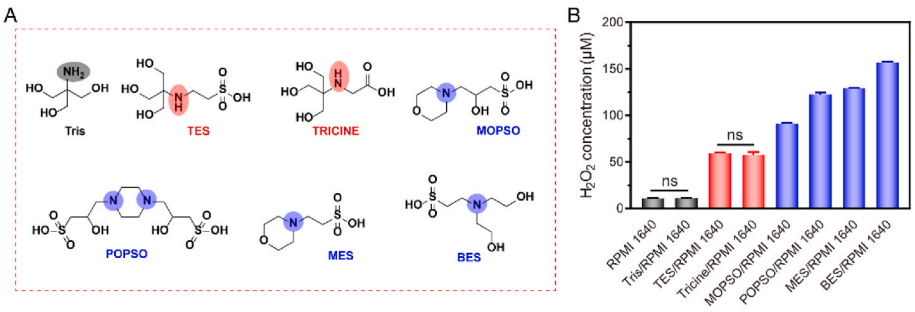

Fig. 2. Generality of Good's buffers in inducing H_2O_2 formation in RPMI 1640 medium under visible light illumination. **(A)** Chemical structure of representative Good's buffers that contains typical primary amine (Tris), secondary amine (TES and Tricine), and tertiary amine (MOPSO, POPSO, MES, and BES) groups. **(B)** Amount of H_2O_2 produced in RPMI 1640 mediums supplied with 25 mM of different Good's buffers under visible light illumination of the ordinary clean bench (1 mW/cm^2) without cells. RPMI 1640 medium without buffer was set as the negative control. Pairwise comparisons are statistically significant unless denoted as "ns" (not significant) as determined by One-way ANOVA multiple comparison tests.

3.2. *Intracellular ROS production in RPMI 1640 mediums associated with HEPES and zwitterionic polybetaines*

Next, we examined potential intracellular ROS production associated with Good's buffers. As expected, intensive intracellular ROS signal as indicated by fluorescence DCF was detected on L-02 cell lines that cultured in the medium supplied with three tertiary-amine-type Good's buffers (HEPES, POPSO, and MOPSO), while no obvious intracellular ROS signal was detected in the cells that cultured with pristine medium (Fig. 3A & B). Similar results were observed on RAW 264.7 cell line (Fig. S3), indicating the generality of these buffers in inducing the abnormal intracellular ROS production.

To clarify the underlying reason, we analyzed the ingredients of intracellular metabolites of cells that cultured with/without the presence of HEPES by NMR and mass spectrometry. Data clearly show characteristic signals of HEPES in the.

intracellular extracts (chemical shift between 2.7 and 4.0 ppm, denoted as red "▼"in Fig. 3C) as compared to the controls (DMEM and intracellular metabolites extracted from Hela cells that cultured in regular DMEM medium). Mass spectra of the intracellular matrix further evidenced the presence of HEPES in the intracellular extracts (Fig. 3D). These data not only indicated a clear cellular uptake phenomenon of HEPES, more importantly, it questioning the past perception of Good's buffers that no trafficking through cell membranes [5–8]. To identify the major contributor of the significantly up-regulated intracellular ROS production, L-02 cells were cultured in HEPES/RPMI 1640 medium for 24 h, then the culture medium was changed to regular RPMI 1640 medium before the fluorescence staining. Interestingly, only minimal L-02

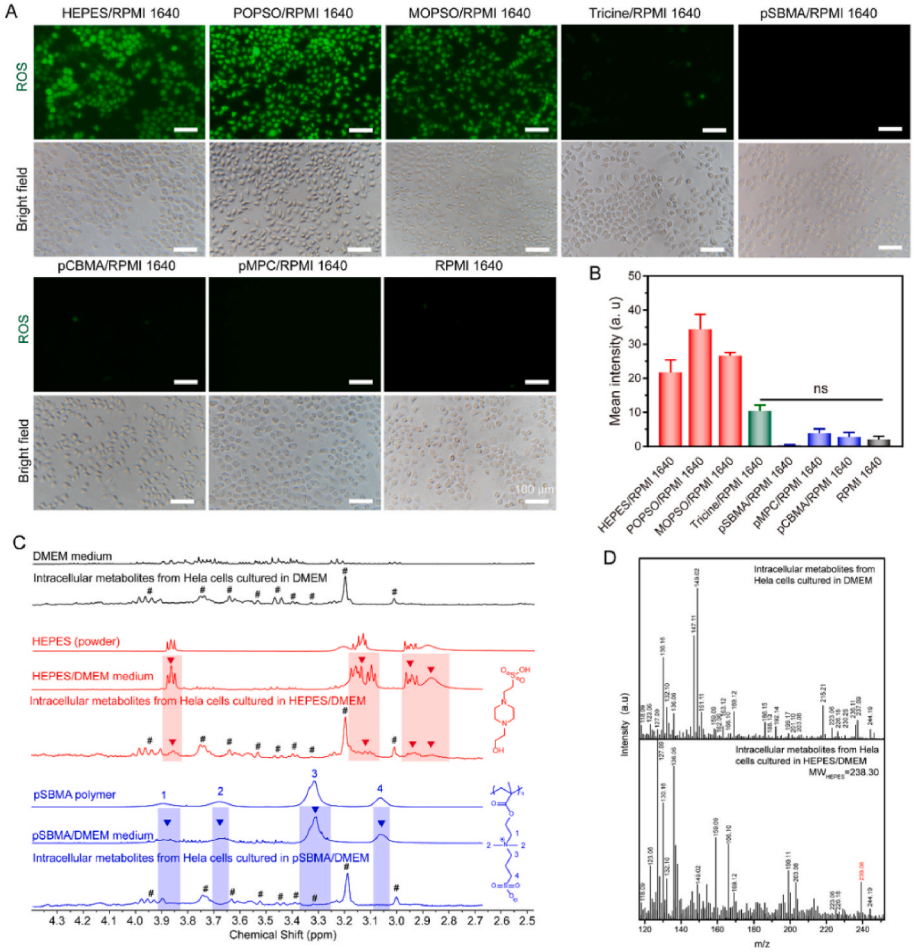

Fig. 3. Cellular uptake phenomenon and intracellular ROS production in the mediums supplied with identical concentration of HEPES and zwitterionic polybetaines under visible light illumination. (A) Fluorescence images and (**B**) fluorescence intensity quantification of the intracellular ROS production in L-02 cells that cultured in RPMI 1640 mediums supplied with different buffers. All scale bars are 100 μm. **(C)** ^{1}H NMR spectra of the intracellular matrix of Hela cells that cultured in DMEM mediums with/without HEPES and zwitterionic polybetaines. "#" means the control signals from the intracellular metabolites while "▼" means the characteristic signals from the corresponding buffering substances. **(D)** Mass spectra of the intracellular matrix extracted from Hela cells that cultured in DMEM mediums with/without HEPES. The signal of HEPES was labeled in red.

cells were stained green (Fig. S4), indicating a slightly up-regulated intracellular ROS production with the HEPES that endocytosed by cells. Therefore, the majority of massive abnormal intracellular ROS detected in cells could be mainly attributed to the penetration of the extracellular H_2O_2 that formed in the medium with the presence of HEPES.

3.3. Disorder of normal cell fate and behaviors that induced by the up-regulated exogenous ROS

ROS play essential roles in cell signaling for it mediates diverse normal cell functions where redox signaling is involved [11,12]. However, it is considered to be a "necessary evil" [12] for cell signaling because the excessive ROS clearly damages DNA, protein and lipid of cells [14]. Therefore, the level of intracellular H_2O_2 is tightly regulated within the range of 0.001–0.7 μM for normal mammalian cells [15], while that of extracellular H_2O_2 is up to 4 μM [15,16]. Given the orders of magnitude elevated abnormal exogenous H_2O_2 formation associated with the presence of HEPES in the culture medium, we further investigated its potential disorder of the normal cell behaviors (cell viability, cytotoxicity, and lysosomal autophagic activation).

To test the potential cytotoxicity of the abnormal exogenous H_2O_2 formed in cell culture medium, the viability of three typical adherent and planktonic cells that cultured with buffered mediums were evaluated. After 3-h's culture in RPMI 1640 mediums supplemented with 25 mM of HEPES, POPSO, MOPOSO, and Tricine, the viabilities of L-02 cells were drastically decreased by approximately 53.8, 77.7, 50.5, 34.4%, respectively ($p < 0.01$, Fig. 4A), while those of RAW 264.7, NB4, A549, and Hela cells were drastically decreased by 83.3, 56.6, 50.3, and 77.8%, respectively ($p < 0.01$, Figs. S5–S7). Confocal microscopy imaging data also confirmed the severe cytotoxicity of the abnormal exogenous H_2O_2 (Fig. 4B and Fig. S8). Further apoptosis assay of L-02 cells indicated the clear damage of the cells (apoptotic cells were stained green, dead cells were stained both green and red, while live cells with no staining) when cultured in the medium that supplied with HEPES as the buffering substances (Fig. S9). The damage of the HEPES to the cells was increased with the prolongation of the regular visible light exposure time, which is consistent to the results of cytocompatibility assays. In vast contrast, zwitterionic pMPC buffers in the RPMI 1640 medium showed no damage to the cells under identical conditions.

To identify the potential impact of HEPES mediated abnormal ROS formation on the lysosomal-autophagic gene network of cells, Ana-1 cells were cultured in RPMI 1640 mediums supplemented with 25 mM of HEPES. Notable activation of the lysosomal-autophagic gene network of the Ana-1 cells was observed (Fig. 4C). Since lysosome is a membrane-bound organelles that is integral to nutrient-sensing and metabolic rewiring [31–33], where ROS is involved for it has been shown to induce autophagy under both physiological and pathological conditions through regulating the multiple MiT-TFE transcription factors including TFEB, TFE3 and MITF [34], as well as activate lysosomal TRPML1 channels (inducing lysosomal Ca^{2+} release) [35]. Further study on RAW 264.7 cells identified that the presence of HEPES in the cell culture medium clearly upregulated the translocation of TFE3, one of representative MiT/TFE transcription factors. In vast contrast, the zwitterionic pMPC buffers showed no difference to that of the negative control group (Fig. 4D). These data clearly indicated the abnormal extracellular & intracellular ROS formation could be the explanation for the irregular lysosomal-autophagic gene network activation of Ana-1 cells that found by Eijk et al. [10].

Given the facts that the exogenous H_2O_2 were converted from the primary ROS ($^1O_2$, ·OH, and $O_2^{\bullet-}$), the higher reactivity of $^1O_2$ than H_2O_2 and comparable moderate reactivity between H_2O_2, ·OH, and $O_2^{\bullet-}$, why the primary ROS in pristine medium showed no obvious up-regulation of extracellular/intracellular ROS production, no cytotoxic, and no lysosomal-autophagic gene network, while the resulting abnormal exogenous H_2O_2 induced systematic side effects? To answer this question, the varied half-life and diffusion distance of different ROS should be taken into account. It's reported that the half-lives of the three

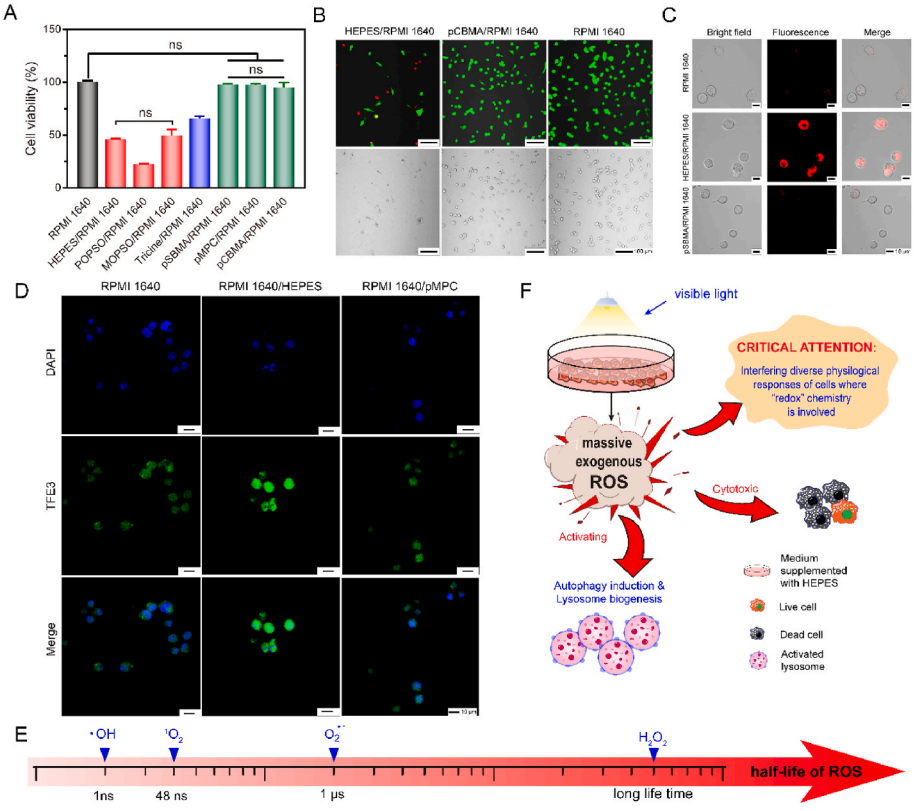

Fig. 4. Disorder of normal cell fate and behavior that induced by the up-regulated exogenous ROS associated with HEPES. (A) Viability of L-02 cells cultured in RPMI 1640 mediums that supplied with 25 mM of representative Good's buffers (HEPES, POPSO, MOPSO, and Tricine) and zwitterionic polybetaines (pSBMA, pMPC, and pCBMA). RPMI 1640 medium without buffer was set as the negative control. **(B)** Live/Dead staining of L-02 cells cultured in HEPES/RPMI 1640 and pCBMA/RPMI 1640 mediums under visible light illumination of the ordinary clean bench (1 mW/cm^2, 3 h). All scale bars are 100 μm. **(C)** LysoTrackerRed staining of Ana-1 cells that cultured in RPMI 1640 mediums supplied with different buffers (HEPES *v.s.* pSBMA). All scale bars are 10 μm. **(D)** Immunofluorescence staining of RAW264.7 cells that cultured in RPMI 1640 mediums supplied with identical concentration of HEPES and pMPC buffers (25 mM). **(E)** Log-plot of the half-life of $^1O_2$, ·OH, $O_2^{\bullet-}$, and H_2O_2. **(F)** Schematic illustration of systematic disorder of cell fate and behavior that induced by the massive exogenous ROS associated with HEPES.

primary ROS ($^1O_2$, ·OH, and $O_2^{\bullet-}$) are ranging from 1 ns to 1 μs (Fig. 4E, Table 1) [23,24,36], therefore, it presumably acts where it was generated (e. g. the diffusion distance of $^1O_2$ is only 20 nm) [36]. In vast contrast, H_2O_2 is a long-life time ROS with much longer diffusion distances, it even can pass through cell membranes freely [37]. The orders of magnitude increased half-life, diffusion distance, and concentration of ROS can undoubtedly produce severe cellular damage and disordering of normal cell functions. Given the facts that endogenous ROS mediate diverse physiological responses such as cell proliferation, differentiation, migration, and metabolism [12], the disordering of cellular fate and behavior by the massive exogenous H_2O_2 is anticipated to be systematic (Fig. 4F) and may produce fundamental fake results in cell based researches. In light of wide presence of tertiary amine structure in Good's buffers, as well as the widespread applications of Good's buffers in cell/tissue culture, virus identification, vaccine manufacture, and protein/tissue storage over the past half a century, these findings call critical attention on the utilization of HEPES and other derived Good's buffers for biological applications.

3.4. Zwitterionic betaines as the new generation biocompatible pH buffers

It's well known that RF is a water soluble vitamin that functions as a prosthetic group of flavoproteins. It could bind macromolecules such as serum albumin in cell culture mediums and plays a role in energy production in the cell/body, thus, RF is widely presented in commercial cell culture mediums. In order to avoid the severe side effects as revealed above that associated with RF and HEPES, we are trying to design a new type of biocompatible buffering substances alternative to HEPES for cell culture.

Zwitterionic betaine-based polymers, including pSBMA, pMPC and pCBMA (Fig. 1A), have attracted substantial attention in the past two decades for their excellent blood compatibility and antifouling capability [38–44]. Based on the revealing of the mechanism why the presence of HEPES in the cell culture medium can induce severe side effects and the understanding of the central role of the tertiary amine structure in mediating massive exogenous H_2O_2 production in the presence of primary ROS, combined with the fact that similar chemical structures between zwitterionic polybetaines and HEPES (contains both positive and negative motifs), we further hypothesize that the zwitterionic polybetaines might be a potential alternative cytocompatible buffering materials. To test this hypothesis, three zwitterionic polybetaines (pSBMA, pMPC, and pCBMA) were prepared (Figs. S10–S12 and Table S1). The extracellular & intracellular ROS production, cellular uptake phenomenon, disordering of the normal cell fate and behaviors, as well as the buffering capacity were evaluated.

As expected, only 7.8, 9.5, and 8.5 μM of H_2O_2 (the same level as compared to that of pristine RPMI 1640 medium) were detected in pSBMA, pMPC and pCBMA containing RPMI 1640 mediums (Fig. 1B) with a time and concentration independent manner (Fig. 1D and **E**), clearly indicating the inertness of zwitterionic polymers in inducing the extracellular H_2O_2 formation in the presence of primary ROS (Fig. 1F). Meanwhile, no obvious intracellular ROS was detected in the cells that cultured with all three zwitterionic polymers supplied mediums (Fig. 3A & B, and Fig. S3), while no obvious cellular uptake was detected (Fig. 3C and Fig. S13). Endocytosis is a basic & complex cellular process that regulates the internalization of diverse molecules. It can be divided into clathrin-dependent and clathrin-independent pathways [45]. However, no matter which pathway takes place, specific interactions between targeting substances and the cell membrane is expected.

Zwitterionic betaine-based polymers are well-known for their excellent antifouling capability [40–44,46,47]. The unique zwitterionic structure (oppositely charged yet overall electronically neutral) is able to bind massive water through electrostatic interactions, forming a steric barrier to interact with proteins and maintaining the normal conformation of proteins that encountered [48,49]. Therefore, without specific interaction or binding with proteins and other biomacromolecules in general, zwitterionic polymers are able to inhibit cellular uptake. Without the production of extra exogenous H_2O_2, the supplement of zwitterionic polymers in the culture medium do not compromise the cell viability (Fig. 4A & B and Figs. S5–S8), and do not up-regulate lysosomal-autophagic gene network activation (Fig. 4C & D, and Fig. S14). These data clearly indicated the advantages of zwitterionic polybetaines over the HEPES or other derived Good's buffers in terms of biocompatibility. Encouraged by these exciting results, we further tested the buffering capacity of the zwitterionic polybetaines.

To investigate the buffering property, stock solutions of three zwitterionic polymers and HEPES were prepared with identical concentrations (0.21 M) and pH (7.0). By constant adding (200 μL/min) of a standard acidic solution (pH = 3.0), the real-time pH of the buffer solutions was monitored. As expected, owing to the capability of zwitterionic motifs to trap H^+ and OH^- ions, three zwitterionic polymers exhibited clear buffering capabilities as compared to the control (Fig. 5A). Further calculation of the Van Slyke buffering index (β_A) [28,29] revealed the buffering capacity order of three zwitterionic polymers: pCBMA > pMPC > pSBMA (Fig. 5A, Fig. S15 and Table 2). Given their similar positively charged structure (quaternary ammonium group), the different buffering capacity could be attributed to varied negatively charged structures of the zwitterionic polymers (carboxylate *v.s.* phosphate *v.s.* sulfonate, Fig. 1A). It is reported that the acid dissociation constant (pK_a) of carboxylate, phosphate and sulfonate groups are 4.76, 1.39 and 1, respectively [50–52]. The higher pK_a value, the greater protonation capability (trapping the H^+ ions) of the compound.

Notably, pCBMA possesses the highest buffering capacity (8.99×10^{-6} mol·pH^{-1}) among the three zwitterionic polymers, however, it was still an order of magnitude lower than that of HEPES at the adjusted initial pH (7.00) condition (Table 2). Multiple protonation groups (two tertiary amine groups and a sulfonate group, Fig. 5B) of HEPES with a higher pK_a value (7.55) [2] could be the underlying reason. Interestingly, without initial adjustment of pH, the buffering index of HEPES (initial pH is 5.40) decreased significantly to 3.98×10^{-5} mol·pH^{-1} (Fig. S16 and Table 2): an order of magnitude lower than that with the initial pH adjustment to 7.0 (Fig. 5C). Instead, the logarithmic value of the acid buffering index (β_A) of pCBMA (initial pH is 5.13) was increased from −5.05 to −3.94 (Table 2). The variations of the buffering capacity along with the adjustment of pH, may be associated with the optimal buffering range of different buffers [53]. Combined with the higher logarithmic value of base buffering index (β_B) than that of HEPES (−5.55 *v.s.* −5.99), pCBMA exhibited an overall better intrinsic buffering capacity than HEPES. Further investigation revealed that the buffer index of pCBMA polymer is proportional to its concentration (Figs. S17A–C and Table 2), indicating the possibility to improve the buffering property by increasing the concentration when required. These data clearly indicated that the zwitterionic polymers, owing to the capacity to trap surrounding H^+ or OH^- ions through electronic interactions, can exhibit comparable buffering properties to that of HEPES.

To validate the pH buffering performance of zwitterionic polymer buffers during cell culture, Hela cells were cultured in DMEM medium that supplied with different buffers in sealed cell culture flasks (Fig. S17D) and the pH variations of the mediums were recorded daily. As expected, the pH of the pristine DMEM was markedly dropped from 7.2 to 7.06 at day 1 while the final pH was decreased by 0.18 pH unit at day 3 (Fig. 5D). In comparison, the significantly minimized pH variations were observed at days 3 on HEPES/DMEM medium (0.06 unit decrease) and pCBMA/DMEM mediums (0.10 and 0.09 unit decrease for 25 and 50 mM, respectively), further confirmed comparable buffering properties of zwitterionic pCBMA and HEPES for cell culture.

To further demonstrate the generality of betaine based materials as the new type of cytocompatible buffering substances, four small molecular zwitterionic betaines were prepared (Fig. 6A). The visible-light induced H_2O_2 production, cellular uptake phenomenon, potential disorder of cellular behaviors, and buffering property of these small molecular betaines were investigated. Interestingly, unlike that of

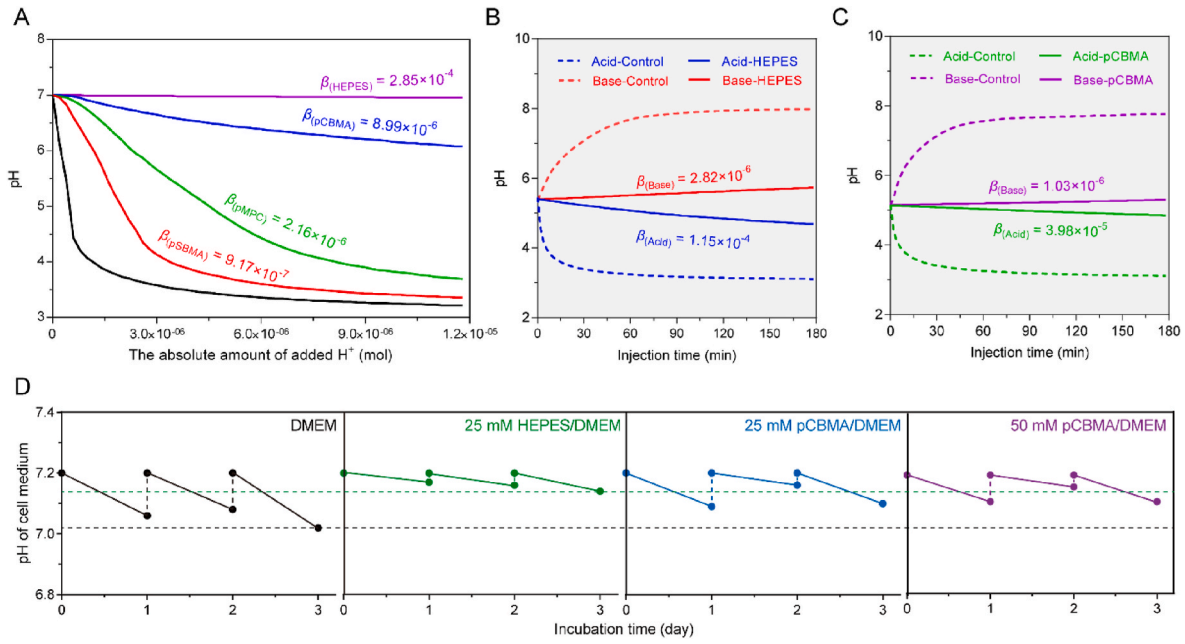

Fig. 5. pH Buffering property of HEPES and zwitterionic polybetaines. (A) Real-time pH monitoring of HEPES, pSBMA, pMPC, and pCBMA aqueous solutions with the adding of standard acidic solution (pH = 3.0) at a constant rate of 200 μL/min. Concentrations of different buffer solutions were fixed at 25 mM with initial pH adjustment to 7.00. Pure water (black curve) was set as the negative control. **(B & C)** Real-time pH monitoring of HEPES and pCBMA aqueous solutions with the adding of standard acidic solution (pH = 3.0) or standard base solution (pH = 9.0) at a constant rate of 200 μL/min. Concentrations of the buffer solutions were fixed at 25 mM without initial pH adjustment. **(D)** pH variations of the culture mediums supplied with different buffers. About 200,000 Hela cells were seeded in each culture bottle. Cell culture mediums were changed daily with corresponding fresh mediums (pH was adjusted to 7.2). DMEM without buffers was set as the negative control.

Table 2
Buffering capacity of various buffers in different conditions.

Buffers	Concentration (mM)	Ttitration standard solution	β (mol·pH^{-1})	$\log_{10}\beta$
pSBMA [a]	210	Acid	9.17×10^{-7}	−6.04
pMPC [a]	210	Acid	2.16×10^{-6}	−5.67
pCBMA [a]	210	Acid	8.99×10^{-6}	−5.05
HEPES [a]	210	Acid	2.85×10^{-4}	−3.55
HEPES [b]	210	Acid	3.98×10^{-5}	−4.40
		Base	1.03×10^{-6}	−5.99
pCBMA [b]	210	Acid	1.15×10^{-4}	−3.94
		Base	2.82×10^{-6}	−5.55
pCBMA	25	Acid	3.47×10^{-6}	−5.46
pCBMA	50	Acid	4.34×10^{-6}	−5.36
pCBMA	100	Acid	6.27×10^{-6}	−5.20
pCBMA	200	Acid	1.22×10^{-5}	−4.91
pCBMA	400	Acid	2.1×10^{-5}	−4.68

[a] initial pH of the buffering solution was adjusted to 7.00.
[b] pristine buffering solution without initial pH adjustment.

macromolecular polybetaines, characteristic signals of all four small molecular betaines were detected from the NMR spectra of intracellular metabolites from Hela cells (Fig. 6B and Fig. S18). This could be mainly attributed to the penetration of the small molecular compounds during the culture similar to that of HEPES [8]. However, all four small molecular betaines did not induce abnormal H_2O_2 production (Fig. 6C) for quaternized amines are inert in inducing H_2O_2 formation in the presence of primary ROS (Fig. 1F). Consequently, all four small molecular betaines showed no compromising of cell viability (Fig. 6D), no abnormal lysosomal-autophagic gene network activation of RAW264.7 cells (Fig. 6E and Fig. S19), and no abnormal intracellular ROS expression (Fig. S20), while exhibited apparent buffering properties (Fig. 6F).

4. Conclusions

For the first time, we have clearly revealed the underlying mechanism that associated with the severe side effects of HEPES during cell culture: RF in the commercial cell culture medium can generate multiple short half-life time ROS (include $^1O_2$, ·OH, and $O_2^{\bullet -}$) under visible light exposure during regular in-door cell manipulation. The tertiary amine group of HEPES turns the majority of these short half-life time ROS to long life-time H_2O_2 with orders of magnitude up-regulated dosages. The massive exogenous ROS not only generate severe cellular damage, but also cause systematic interfering to the redox signaling of cells (e. g. lysosomal-autophagic gene network activation of cells) and may produce fundamental fake results in cell based researches.

More importantly, we have illustrated the generality of Good's buffers in inducing abnormal exogenous H_2O_2 formation in cell culture mediums, and further revealed an order of tertiary amines > secondary amines > primary amines in term of the capacity to induce H_2O_2 formation under identical conditions. Given the facts that endogenous ROS mediate diverse physiological responses (e. g. cell proliferation, differentiation, migration, and metabolism) and the wide presence of tertiary amine and secondary amine structures in Good's buffers, these findings call critical attention on the use of Good's buffers for biological applications.

Based on the understanding of the above mechanism, we have further designed and validated zwitterionic betaine based materials as an alternative cytocompatible buffers. Its quaternized amine group, over the tertiary amine groups in HEPES, is able to completely avoid the abnormal extracellular and intracellular ROS production and the consequent systematical severe side effects that found on HEPES. Meanwhile, its unique oppositely charged yet overall electronically neutral structures can effectively trap the surrounding free H^+ or OH^- ions, endowing comparable buffering capacity to HEPES. These findings may enable zwitterionic betaines as the leading biocompatible & the new generation organic pH buffering materials for a wide range of

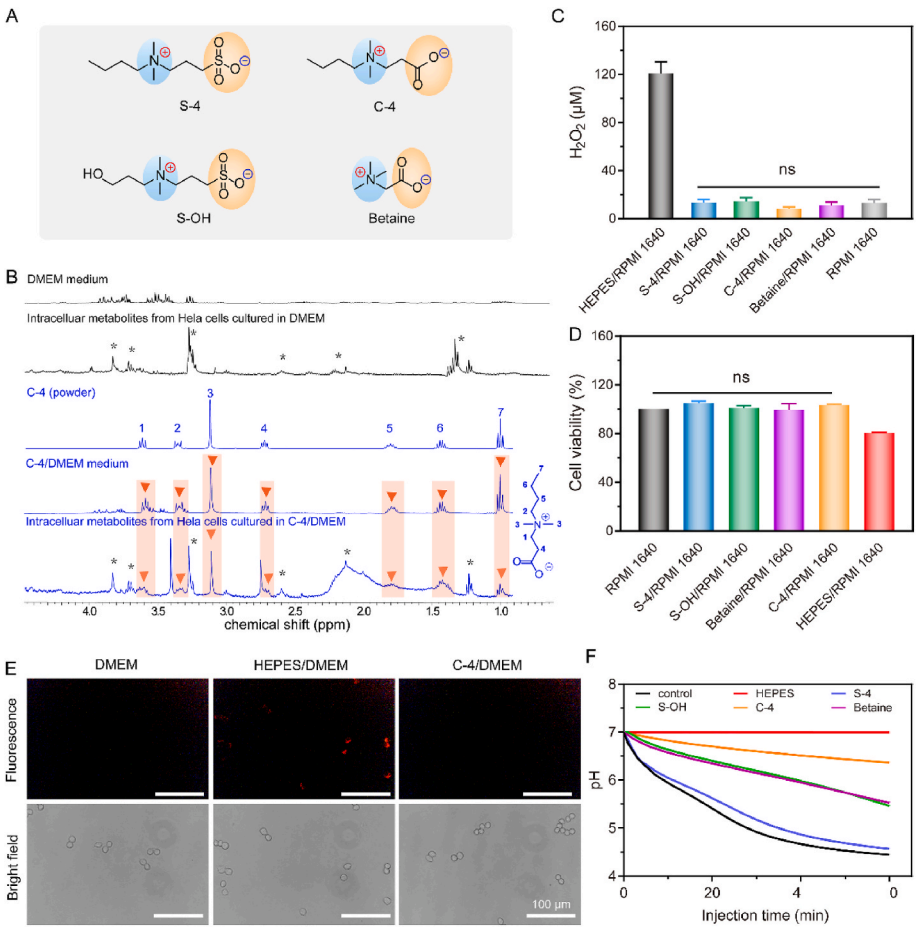

Fig. 6. H_2O_2 production, cellular uptake phenomenon, disorder of cellular behavior, and buffering property of small molecular betaines. (**A**) Chemical structures of small molecular zwitterionic sulfobetaines (S-4 and S–OH) and carboxybetaine (C-4 and betaine). (**B**) ^{1}H NMR spectra of the intracellular matrix of Hela cells that cultured in DMEM mediums with C-4. "#" means the control signals from the intracellular metabolites while "▼" means the characteristic signals from the corresponding buffering substances. (**C**) Amount of H_2O_2 formed in RPMI 1640 mediums supplied with 25 mM of small molecular zwitterionic betaines under simulated sunlight illumination without cells. RPMI 1640 medium without buffer was set as the negative control. (**D**) Viability of L-02 cells cultured in RPMI 1640 mediums that supplied with 25 mM of HEPES and small molecular zwitterionic betaines. (**E**) LysoTrackerRed staining of RAW264.7 cells that cultured in DMEM mediums supplied with different buffers (HEPES *v.s.* C-4). All scale bars are 100 μm. (**F**) Real-time pH monitoring of small molecular zwitterionic betaines aqueous solutions with the adding of standard acidic solution (pH = 4.0) at a constant rate of 200 μL/min. Concentrations of different buffer solutions were fixed at 100 mM with initial pH adjustment to 7.00. Pure water (black curve) was set as the negative control. Pairwise comparisons are statistically significant unless denoted as "ns" (not significant) as determined by One-way ANOVA multiple comparison tests.

biomedical applications. These findings may also open a new avenue for zwitterionic betaine based materials for biomedical applications.

This is a primary study to announce a critical attention of HEPES as the pH buffer for cell culture and propose the zwitterionic betaine based materials as the potential alternative pH buffering substance for cell culture. Many further investigations such as the disordering of normal functions of many other cell lines, as well as the deep & detailed researches regarding how these buffering substances impact the signal pathways, the function of organelle, and the consequent metabolism process of any specific cells are worthy of study.

Ethics approval and consent to participate

No human or animal model, no human or animal tissue was used in the current study.

CRediT authorship contribution statement

Peiming Liu: Writing – original draft, designed the preparation of the zwitterionic polymers and small molecular zwitterionic betaines, the buffering capacity, cellular uptake, lysosomal activation, and in vivo implantation experiments, analyzed the data, contributed to the writing of the original manuscript. **Jin Sun:** designed the H2O2 formation identification and cell viability experiments, performed the H2O2 formation identification and cell viability experiments, analyzed the data, contributed to the editing of the manuscript. **Wan Peng:** performed the cell apoptosis experiments, analyzed the data. **Yahui Gu:** performed the above experiments, analyzed the data, contributed to the editing of the manuscript. **Xiaoxue Ji:** assisted cell viability experiment. **Zhi Su:** supported partial of cell viability experiment and discussed the data. **Pingsheng Liu:** Writing – original draft, conceived the project, designed the preparation of the zwitterionic polymers and small molecular zwitterionic betaines, the buffering capacity, cellular uptake, lysosomal activation, and in vivo implantation experiments, designed the H2O2 formation identification and cell viability experiments, analyzed the data, contributed to the writing of the original manuscript, contributed to the editing of the manuscript. **Jian Shen:** conceived the project.

Declaration of competing interest

The authors declare the following financial interests/personal relationships which may be considered as potential competing interests: P. S. Liu, J. Shen, P.M. Liu and J. Sun are inventors of a patent application (China patent 202010348733X) that covers the zwitterionic betaine based buffers.

Acknowledgments

We thank the grant support from National Natural Science Foundation of China (No. 21504046), Natural Science Foundation of Jiangsu Province (No. BK20150970), the Six Talent Peaks Project in Jiangsu Province (SWYY-060), and the Projects of Nanjing Normal University (No. 184080H20192; 184080H10386).

Appendix A. Supplementary data

Supplementary data to this article can be found online at https://doi.org/10.1016/j.bioactmat.2022.12.028.

References

[1] A. Fisk, S. Pathak, HEPES-buffered medium for organ culture, Nature 224 (1969) 1030–1031.
[2] H. Eagle, Buffer combinations for mammalian cell culture, Science 174 (4008) (1971) 500–503.
[3] C. Ceccarini, H. Eagle, pH as a determinant of cellular growth and contact inhibition, Proc. Natl. Acad. Sci. USA 68 (1) (1971) 229–233.
[4] M. Oginuma, Y. Harima, O.A. Tarazona, M. Diaz-Cuadros, A. Michaut, T. Ishitani, F. Xiong, O. Pourquie, Intracellular pH controls WNT downstream of glycolysis in amniote embryos, Nature 584 (7819) (2020) 98–101.
[5] N.E. Good, G.D. Winget, W. Winter, T.N. Connolly, S. Izawa, R.M. Singh, Hydrogen ion buffers for biological research, Biochemistry 5 (2) (1966) 467–477.
[6] C. Shipman, Evaluation of 4-(2-hydroxyethyl)-1-piperazineëthanesulfonic acid (HEPES) as a tissue culture buffer, Proc. Soc. Exp. Biol. Med. 130 (1) (1968) 305–310.
[7] R.E. Weber, Use of ionic and zwitterionic (Tris BisTris and HEPES) buffers in studies on hemoglobin function, J. Appl. Physiol. 72 (4) (1992) 1611–1615.
[8] R. Depping, K. Seeger, (1)H-NMR spectroscopy shows cellular uptake of HEPES buffer by human cell lines-an effect to be considered in cell culture experiments, Anal. Bioanal. Chem. 411 (4) (2019) 797–802.
[9] J.S. Zigler Jr., J.L. Lepe-Zuniga, B. Vistica, I. Gery, Analysis of the cytotoxic effects of light-exposed HEPES-containing culture medium, Vitro Cell Dev. Biol. 21 (5) (1985) 282–287.
[10] M.J. Tol, M.J.C. van der Lienden, T.L. Gabriel, J.J. Hagen, S. Scheij, T. Veenendaal, J. Klumperman, W.E. Donker-Koopman, A.J. Verhoeven, H. Overkleeft, J.M. Aerts, C.A. Argmann, M. van Eijk, HEPES activates a MiT/TFE-dependent lysosomal-autophagic gene network in cultured cells: a call for caution, Autophagy 14 (3) (2018) 437–449.
[11] H.A. Woo, S.H. Yim, D.H. Shin, D. Kang, D.Y. Yu, S.G. Rhee, Inactivation of peroxiredoxin I by phosphorylation allows localized H2O2 accumulation for cell signaling, Cell 140 (4) (2010) 517–528.
[12] S.G. Rhee, H2O2, a necessary evil for cell signaling, Science 312 (5782) (2006) 1882–1883.
[13] T. Finkel, Signal transduction by reactive oxygen species, J. Cell Biol. 194 (1) (2011) 7–15.
[14] Y.S. Bae, H. Oh, S.G. Rhee, Y.D. Yoo, Regulation of reactive oxygen species generation in cell signaling, Mol. Cell 32 (6) (2011) 491–509.
[15] J.R. Stone, S.P. Yang, Hydrogen peroxide: a signaling messenger, Antioxidants Redox Signal. 8 (3–4) (2006) 243–270.
[16] N.V. Kulagina, A.C. Michael, Monitoring hydrogen peroxide in the extracellular space of the brain with amperometric microsensors, Anal. Chem. 75 (18) (2003) 4875–4881.
[17] M. Kirsch, E.E. Lomonosova, H.G. Korth, R. Sustmann, H. de Groot, Hydrogen peroxide formation by reaction of peroxynitrite with HEPES and related tertiary amines. Implications for a general mechanism, J. Biol. Chem. 273 (21) (1998) 12716–12724.
[18] A. Grzelak, B. Rychlik, G. Baptosz, Light-dependent generation of reactive oxygen species in cell culture media, Free Radic. Biol. Med. 30 (12) (2001) 1418–1425.
[19] P.E. Hockberger, T.A. Skimina, V.E. Centonze, C. Lavin, S. Chu, S. Dadras, J. K. Reddy, J.G. White, Activation of flavin-containing oxidases underlies light-induced production of H_2O_2 in mammalian cells, Proc. Natl. Acad. Sci. USA 96 (11) (1999) 6255–6260.
[20] L.L. Ingraham, D.L. Meyer, Biochemistry of Dioxygen, Plenum Press, New York, 1985.
[21] P.R. Ogilby, Singlet oxygen: there is indeed something new under the sun, Chem. Soc. Rev. 39 (8) (2010) 3181–3209.
[22] Q. Zheng, X. Liu, Y. Zheng, K.W.K. Yeung, Z. Cui, Y. Liang, Z. Li, S. Zhu, X. Wang, S. Wu, The recent progress on metal-organic frameworks for phototherapy, Chem. Soc. Rev. 50 (8) (2021) 5086–5125.
[23] P. Pieta, A. Petr, W. Kutner, L. Dunsch, In situ ESR spectroscopic evidence of the spin-trapped superoxide radical, O_2^-, electrochemically generated in DMSO at room temperature, Electrochim. Acta 53 (8) (2008) 3412–3415.
[24] W. Stahl, H. Sies, Antioxidant defense: vitamins E and C and carotenoids, Diabetes 46 (Supplement 2) (1997) S14–S18.
[25] Z. Zhang, T. Chao, S.F. Chen, S.Y. Jiang, Superlow fouling sulfobetaine and carboxybetaine polymers on glass slides, Langmuir 22 (24) (2006) 10072–10077.
[26] T. Huang, H.W. Liu, P.M. Liu, P.S. Liu, L. Li, J. Shen, Zwitterionic copolymers bearing phosphonate or phosphonic motifs as novel metal-anchorable anti-fouling coatings, J. Mater. Chem. B 5 (27) (2017) 5380–5389.
[27] C. Gey, K. Seeger, Metabolic changes investigated by proton NMR spectroscopy in cells undergoing oncogene-induced senescence, Methods Mol. Biol. 1534 (2017) 155–163.
[28] D. Donald, S. Van, On the measurement of buffer values and on the relationship of buffer value to the dissociation constant of the buffer and the concentration and reaction of the buffer solution, J. Biol. Chem. 52 (2) (1922) 525–570.
[29] J. Butcher, Q. Fernando, Use of a digital computer in equilibrium calculations: the effects of dilution and ionic strength of the buffer index and sharpness index in the titration of a monoprotic acid with a strong base, Anal. Chim. Acta 36 (1966) 65–76.
[30] V. Chiriac, G. Balea, Buffer index and buffer capacity for a simple buffer solution, J. Chem. Educ. 74 (8) (1997) 937–939.
[31] R. Perera, S. Stoykova, B.N. Nicolay, K.N. Ross, J. Fitamant, M. Boukhali, J. Lengrand, V. Deshpande, M.K. Selig, C.R. Ferrone, J. Settleman, G. Stephanopoulos, N.J. Dyson, R. Zoncu, S. Ramaswamy, W. Haas, N. Bardeesy, Transcriptional control of autophagy-lysosome function drives pancreatic cancer metabolism, Nature 524 (7565) (2015), 361-U251.
[32] A. Folick, H.D. Oakley, Y. Yu, E.H. Armstrong, M. Kumari, L. Sanor, D.D. Moore, E. A. Ortlund, R. Zechner, M.C. Wang, Lysosomal signaling molecules regulate longevity in Caenorhabditis elegans, Science 347 (6217) (2015) 83–86.
[33] C. Settembre, A. Fraldi, D.L. Medina, A. Ballabio, Signals from the lysosome: a control centre for cellular clearance and energy metabolism, Nat. Rev. Mol. Cell Biol. 14 (5) (2013) 283–296.
[34] H. Wang, N. Wang, D. Xu, Q. Ma, Y. Chen, S. Xu, Q. Xia, Y. Zhang, J.H.M. Prehn, G. Wang, Z. Ying, Oxidation of multiple MiT/TFE transcription factors links oxidative stress to transcriptional control of autophagy and lysosome biogenesis, Autophagy 16 (9) (2020) 1683–1696.
[35] X.L. Zhang, X.P. Cheng, L. Yu, J.S. Yang, R. Calvo, S. Patnaik, X. Hu, Q. Gao, M. M. Yang, M. Lawas, M. Delling, J. Marugan, M. Ferrer, H.X. Xu, MCOLN1 is a ROS sensor in lysosomes that regulates autophagy, Nat. Commun. 7 (2016).
[36] Q. Zheng, X. Liu, Y. Zheng, K.W.K. Yeung, Z. Cui, Y. Liang, Z. Li, S. Zhu, X. Wang, S. Wu, The recent progress on metal-organic frameworks for phototherapy, Chem. Soc. Rev. 50 (8) (2021) 5086–5125.
[37] I. Slesak, M. Libik, B. Karpinska, S. Karpinski, Z. Miszalski, The role of hydrogen peroxide in regulation of plant metabolism and cellular signalling in response to environmental stresses, Acta Biochim. Pol. 54 (1) (2007) 39–50.
[38] P. Zhang, F. Sun, C. Tsao, S. Liu, P. Jain, A. Sinclair, H. Hung, T. Bai, K. Wu, S. Jiang, Zwitterionic gel encapsulation promotes protein stability, enhances pharmacokinetics, and reduces immunogenicity, Proc. Natl. Acad. Sci. U.S.A. 112 (39) (2015) 12046–12051.
[39] P. Liu, Q. Chen, S. Wu, J. Shen, S. Lin, Surface modification of cellulose membranes with zwitterionic polymers for resistance to protein adsorption and platelet adhesion, J. Membr. Sci. 350 (1–2) (2010) 387–394.
[40] P. Liu, Q. Chen, L. Li, S. Lin, J. Shen, Anti-biofouling ability and cytocompatibility of the zwitterionic brushes-modified cellulose membrane, J. Mater. Chem. B 2 (41) (2014) 7222–7231.
[41] A. Erfani, J. Seaberg, C.P. Aichele, J.D. Ramsey, Interactions between biomolecules and zwitterionic moieties: a review, Biomacromolecules 21 (7) (2020) 2557–2573.
[42] A.J. Keefe, S. Jiang, Poly(zwitterionic)protein conjugates offer increased stability without sacrificing binding affinity or bioactivity, Nat. Chem. 4 (1) (2012) 60–64.
[43] L. Zhang, Z. Cao, T. Bai, L. Carr, J.R. Ella-Menye, C. Irvin, B.D. Ratner, S. Jiang, Zwitterionic hydrogels implanted in mice resist the foreign-body reaction, Nat. Biotechnol. 31 (6) (2013) 553–556.
[44] W. Peng, P. Liu, X. Zhang, J. Peng, Y. Gu, X. Dong, Z. Ma, P. Liu, J. Shen, Multi-functional zwitterionic coating for silicone-based biomedical devices, Chem. Eng. J. 398 (2020), 125663.
[45] S. Mayor, R.E. Pagano, Pathways of clathrin-independent endocytosis, Nat. Rev. Mol. Cell Biol. 8 (8) (2007) 603–612.
[46] P. Zhang, F. Sun, C. Tsao, S. Liu, P. Jain, A. Sinclair, H. Hung, T. Bai, K. Wu, S. Jiang, Zwitterionic gel encapsulation promotes protein stability, enhances pharmacokinetics, and reduces immunogenicity, Proc. Natl. Acad. Sci. USA 112 (39) (2015) 12046–12051.
[47] J.F. Jia, H.J. Zhou, J. Wei, X. Jiang, H. Hua, F.P. Chen, S.C. Wei, J.W. Shin, C. S. Liu, Development of magnesium calcium phosphate biocement for bone regeneration, J. R. Soc. Interface 7 (49) (2010) 1171–1180.
[48] H. Yan, H. Zhu, J. Shen, Molecular dynamics simulation study on zwitterionic structure to maintain the normal conformations of Glutathione, Sci. China, Ser. B 50 (5) (2007) 660–664.
[49] K. Ishihara, H. Nomura, T. Mihara, K. Kurita, Y. Iwasaki, N. Nakabayashi, Why do phospholipid polymers reduce protein adsorption? J. Biomed. Mater. Res. 39 (2) (1998) 323–330.
[50] D.H. Ripin, D.A. Evans, pKa's of Inorganic and Oxo-Acids. http://evans.harvard.edu/pdf/evans_pKa_table.pdf, 2005.
[51] D.S. Reichmuth, B.J. Kirby, Effects of ammonioalkyl sulfonate internal salts on electrokinetic micropump performance and reversed-phase high-performance liquid chromatographic separations, J. Chromatogr., A 1013 (1–2) (2003) 93–101.
[52] W.D. Kumler, J.J. Eiler, The acid strength of mono and diesters of phosphoric acid. The n-alkyl esters from methyl to butyl, the esters of biological importance, and the natural guanidine phosphoric acids, J. Am. Chem. Soc. 65 (12) (1943) 2355–2361.
[53] C.M.H. Ferreira, I.S.S. Pinto, E.V. Soares, H.M.V.M. Soares, (Un)suitability of the use of pH buffers in biological, biochemical and environmental studies and their interaction with metal ions - a review, RSC Adv. 5 (39) (2015) 30989–31003.